Distortion and Crack Prediction and Experiments in quenching AISI 4140 C-Rings

da Silva, A. D.[1]
Pedrosa, T. A.[2]
Pereira, P. H. R.[3]
Schillé, J-P.[4]
Guo, Z.[4]
Cetlin, P. R.[1]

[1] *School of Engineering, Federal University of Minas Gerais, Brazil (lissonds@gmail.com).*
[2] *Assistant Researcher, CNEN (Brazilian National Commission of Nuclear Energy), CDTN (Center for the Development of Nuclear Energy).*
[3] *Undergraduate Student, School of Engineering, Federal University of Minas Gerais.*
[4] *JMatPro, Sente Software Ltd,. Surrey Technology Centre, 40 Occam Road, United Kingdom.*

Abstract

For Heat Treatment processes, high cooling rates commonly cause geometric distortions in steel parts, associated with the thermal contraction and with the change in the mechanical and geometrical properties of austenite and martensite. It is of importance to predict the geometric behavior of mechanical components during heat treatment in order to improve the quality of the product, modifying the heat treatment process. This study presents finite element (FE) simulations of the quenching of AISI 4140 steel C-rings in oil and water, which is compared with experimental data. The severity of the water quenching was responsible for the larger simulated distortion when compared with the oil quenching process. Water quenched C-ring crack and the applied residual stresses during the cooling stage were investigated. The simulations were carried out with coupled analysis of heat transfer, deformation mechanics and phase transformations. In addition, hardness and microstructure formation were obtained through numerical simulation.

Keywords: Distortion; crack; quenching; C-ring; FE simulation; 4140 steel; microstructure; hardness.

1 INTRODUCTION

A wide range of mechanical components is produced through forming , which can be followed by heat treatment processes. Quenching is conducted after forming stages of steel parts in order to enhance the material properties of the workpiece, *i.e.*, hardness. However, this process commonly causes undesired geometric distortions in the quenched parts. The dimensional accuracy of these parts is affected and leads to production and economical losses. Various factors including phase transformation of steel, retained austenite, quench media, severity and uniformity and process selection may influence the final dimensions of a quenched part [1,2,3]. As an example, hot rolled and heat treated rings commonly present ovality distortions after quenching process [4].

One way of circumventing the problems connected to the distortion of parts caused by heat treatments is to design adequate post-heat treatment forming operations that would eliminate the distortions. Another possibility is to include straightening processes following heat treatment steps. Both approaches represent fundamental design procedures in order to obtain a final adequate part, and depend on the possibility of predicting accurately the distortions caused by the heat treatments.

The C-ring type test is commonly used to investigate the distortion propensity of materials that undergo heat treatment processes such as quenching [5]. The influence of chemical composition on the hardenability and quench distortion of automotive components has already been investigated [6,7]. Numerical simulations and experimental tests for the quenching of cast steel C-rings were conducted [8], but did not lead to an adequate correlation for the experimental and predicted magnitudes of the distortions. Experimental quenching of C-ring specimens for different materials (including 4140 steel) have been conducted [9,10], and the resulting gap opening and outside diameter of the C-rings have been reported. The simulation of the quenching of C-rings based on 4140 steel material data has been performed, and differences between the results and those reported in the literature were reported [11]. In addition, a good correlation between the simulated and experimental results for quench distortions depends critically on the knowledge of the properties of the materials during their cooling [1].

No satisfactory comparison between numerical simulations and experimental results on the distortion and microstructural and hardness distribution could be found in the literature for quenched 4140 C-rings. The objective of the present work is to define a methodology to predict heat treatment distortion, which might be used to be compared with future experimental procedures, and be extended to approach mechanical components produced by the forging industry. In addition, two different quenching processes are analyzed, oil and water quenching, in order to verify the influence of the quenchant severity in the distortion magnitudes.

2 METHODOLOGY

2.1. Experimental procedure

The material employed for the C-ring was an AISI 4140, with the nominal composition (in wt%, certified by the supplier) of 0.40% C, 0.20% Si, 0.85% Mn, 0.95% Cr, 0.20% Mo. The geometry and dimensions of the C-rings are given in Figure 1.

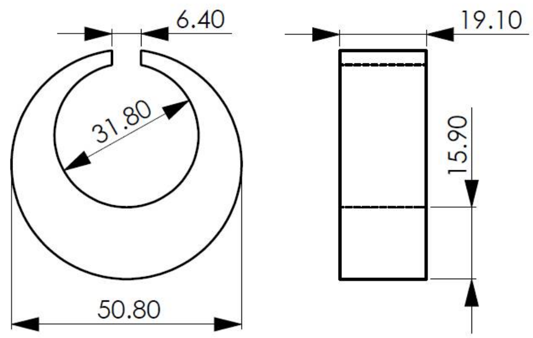

Figure 1 – C-ring geometry (all dimensions in mm).

The measurements of the ring dimensions before and after the heat treatments were performed in a Mitutoyo Shadowgraph PJ A3000 Model with an accuracy of 0.01 mm. Two dimensional changes were analyzed: gap opening, *G*, and outside diameter, *OD*. Based on Figure 2, the dimensional changes may be expressed as:

$$G = n' - n \,, \quad (1)$$

and

$$OD = m' - m \,. \quad (2)$$

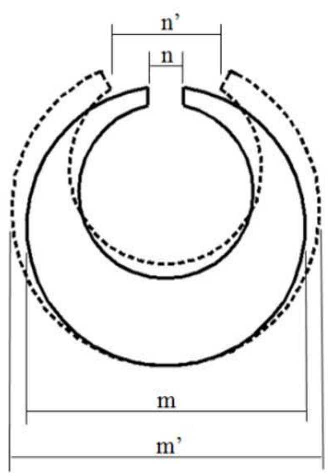

Figure 2 – C-ring specimen before heat treatment (*m* and *n* dimensions) and after heat treatment (*m'* and *n'* dimensions).

The rings were heated to 900 °C in a tubular furnace where an Argon gas flow was maintained for minimizing the oxidation of the material, and held at this temperature for 3600 s in order to attain a homogeneous austenitic microstructure. Quenching was then performed through the fast vertical movement of the ring (thickest part of the ring at the bottom and ring gap at the top) into the quenching oil (CASTROL OILQUENCH 1) at 25 ºC, where it was held for at least 300 s.
The microstructure of the quenched C-rings was evaluated at various points of the longitudinal and transversal cross-sections of the C-rings, as illustrated in Figure 3. Sample preparation involved conventional surface grinding, polishing and etching with Nital 2%. Hardness measurements (HRC – Rockwell "C") were taken at various locations in the sections indicated in Figure 3.

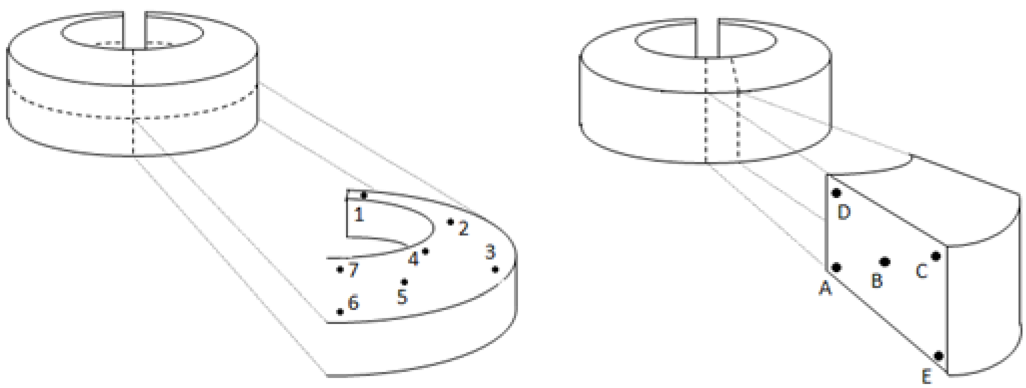

(a) (b)

Figure 3 – Location of the regions where the microstructure of the quenched C-rings was examined (a) in the longitudinal cross-section and (b) in the transversal cross-section.

2.2. Numerical Simulation

The simulations were performed using the software DEFORM^{TM}-HT module, version 10.1 (Scientific Forming Technology Corporation, Columbus, Ohio, USA), based on the Finite Element Method, establishing a coupling between all of the involved phenomena as shown in Figure 4. The part distortion was predicted taking into account the deformation based on the following strain components:

$$d\varepsilon_{ij} = d\varepsilon_{ij}^{e} + d\varepsilon_{ij}^{p} + d\varepsilon_{ij}^{th} + d\varepsilon_{ij}^{tr} + d\varepsilon_{ij}^{tp}, \quad (3)$$

where *e*, *p*, *th*, *tr*, and *tp* represent the contributions from elastic, plastic, thermal, phase transformation and transformation plasticity, respectively.

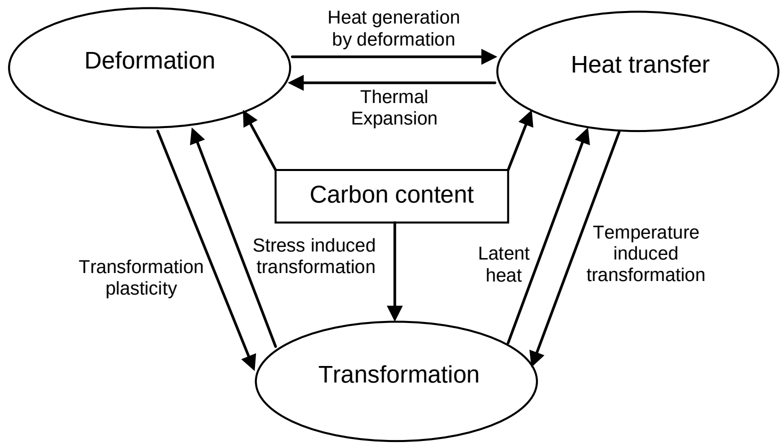

Figure 4 – Coupled phenomena considered during the quenching simulations.

In order to obtain adequate simulation results the material data should be accurate. The following information on materials properties have to be known for distortion prediction caused by quenching through numerical simulations: phase transformation kinetics, *i.e.*, TTT and CCT diagrams; temperature dependent thermo-physical properties for each phase formed, such as density, Young's modulus, thermal expansion coefficient, and thermal conductivity; and temperature dependent mechanical properties of each phase formed, including tensile strength, yield strength, and hardness.

The materials properties required for distortion simulation are calculated using JMatPro, since that the above data involves long and expensive laboratory testing; an alternative is the use of softwares focused on material properties simulation, which are usually based on the chemical composition of the material. As an example of the material models employed by JMatPro, the TTT curves of the 4140 steel are given in Figure 5, where the austenite grain size is taken as ASTM 9 and austenisation temperature taken as 900°C. The linear expansion of alloy 4140 during a thermal cycle is shown in Figure 6, where both heating and cooling rate are set as 10^{o}C/s.

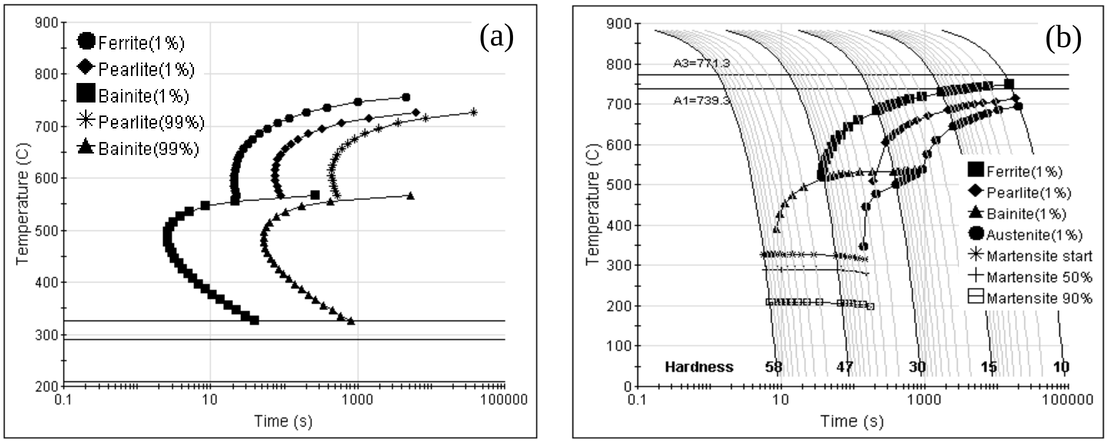

Figure 5 – TTT and CCT diagrams of steel 4140 calculated by JMatPro.

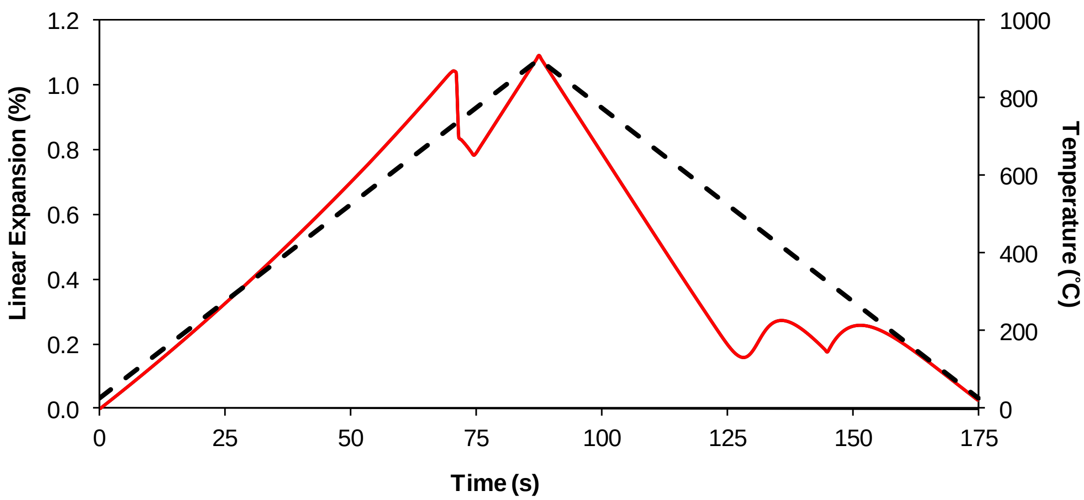

Figure 6 – Linear expansion of alloy 4140 during a heating and cooling cycle, both at 10 °C/s.

The simulation of the C-ring involved the prediction of the ring expansion due to the temperature increase from 20 to 900 °C. The coefficient of thermal expansion for the 4140 steel was obtained from the DEFORM^{TM} library. At 900 °C, the specimen was considered as completely austenitized (100% austenite).

The heat transfer coefficient between AISI 4140 and oil and water quenchants as a function of temperature has already been determined [11], and was used in the present simulation. Figure 7 shows the variation of this coefficient with the specimen surface temperature.

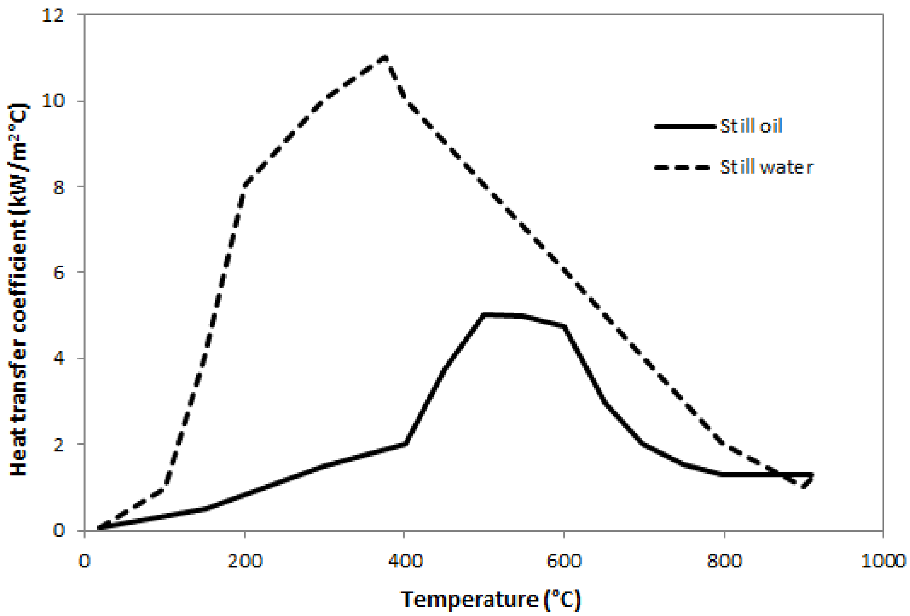

Figure 7 – Heat transfer coefficient between AISI 4140 and two different quenchants: still oil and water [11].

Due to the part symmetry, only ¼ of the part was simulated. Brick elements were used (7,000), as shown in Figure 8. Nodes *M* and *N* were utilized for outside diameter and gap opening measurements, respectively. The microstructure and hardness of the quenched C-rings was evaluated on the cross-sections of the C-rings, as illustrated in Figure 3. Table 1 summarizes the FE setup for the simulations.

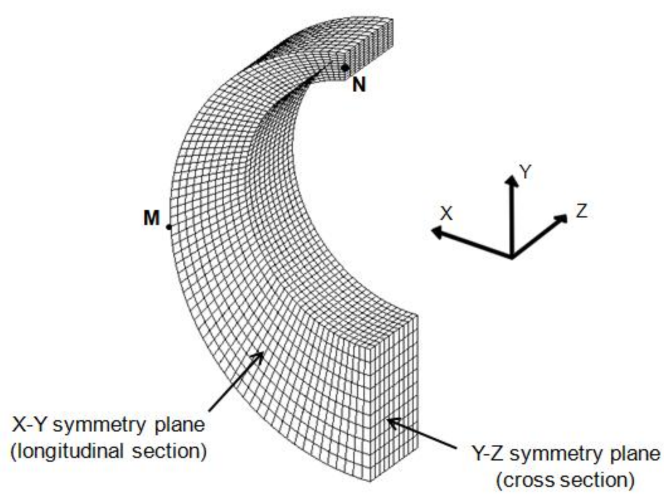

Figure 8 – Meshed ¼ symmetric geometry, used for the simulation. Nodes *M* and *N* were used for outside diameter and gap opening evaluation, respectively.

Table 1 – FE setup for the simulations.

Operation	Parameter	Value
1 – Heating (furnace)	Code	DEFORM-3D™
	C-ring geometry	Figure 1
	Material	AISI 4140 from DEFORM-3D™ library
	Initial temperature	20 °C
	Furnace temperature	900 °C
	Object type	Elastic
2 – Quenching (oil)	Code	DEFORM-3D™
	C-ring geometry	Expanded - Operation 1
	Material	AISI 4140 from JMatPro
	Initial temperature	900 °C
	Quenchant temperature	25 °C
	Heat transfer coefficient	Function of temperature (Figure 5)
	Object type	Elasto-plastic

3 RESULTS AND DISCUSSION

3.1. Distortion of the C-rings

There is a tendency for the “opening” of the ring. Figure 9 displays the simulated displacements in the *x* direction of node *M*, comparing oil and water quenching. In the same way, Figure 10 displays the simulated displacements in the *x* direction of node *N*. The data considers a period of 150 s after the beginning of the quenching process. Considering that a symmetric FE model has been used, the x-displacement given in Figures 9 and 10 represents only half of the total dimensional change. Thus, for the oil quenching process, the ring gap opens 0.40 mm and the outer diameter expands about 0.08 mm. For the water quenching process, the ring gap opens 0.68 mm and the outer diameter expands 0.18 mm. Table 2 presents a comparison between oil and water quench values for the C-ring distortions.

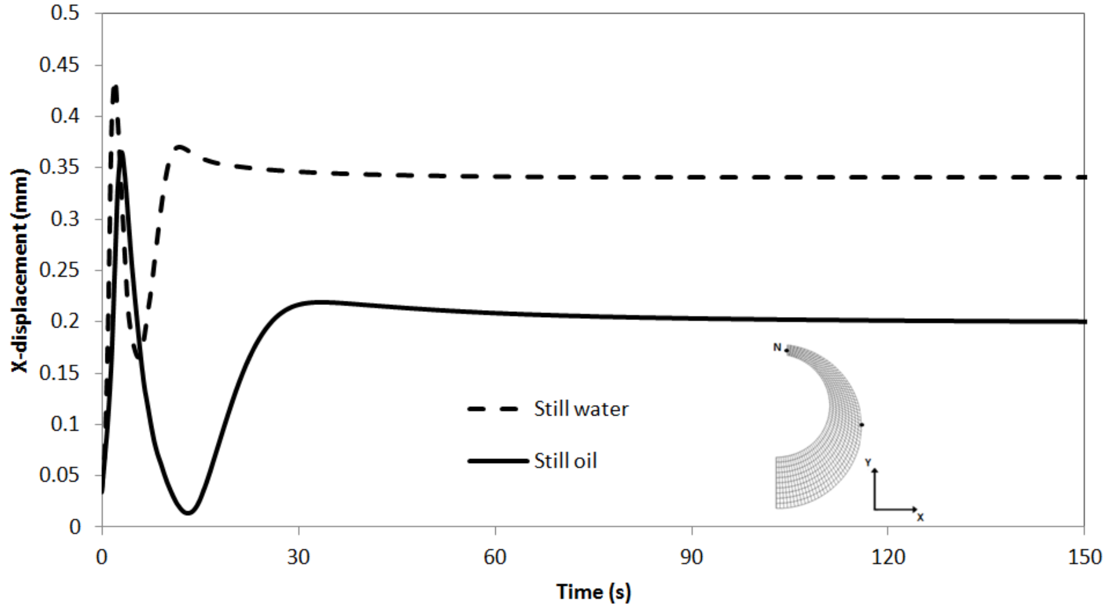

Figure 9 – Simulated displacements in the *x* direction for Node *N* of the C-ring for still oil and water quenching processes.

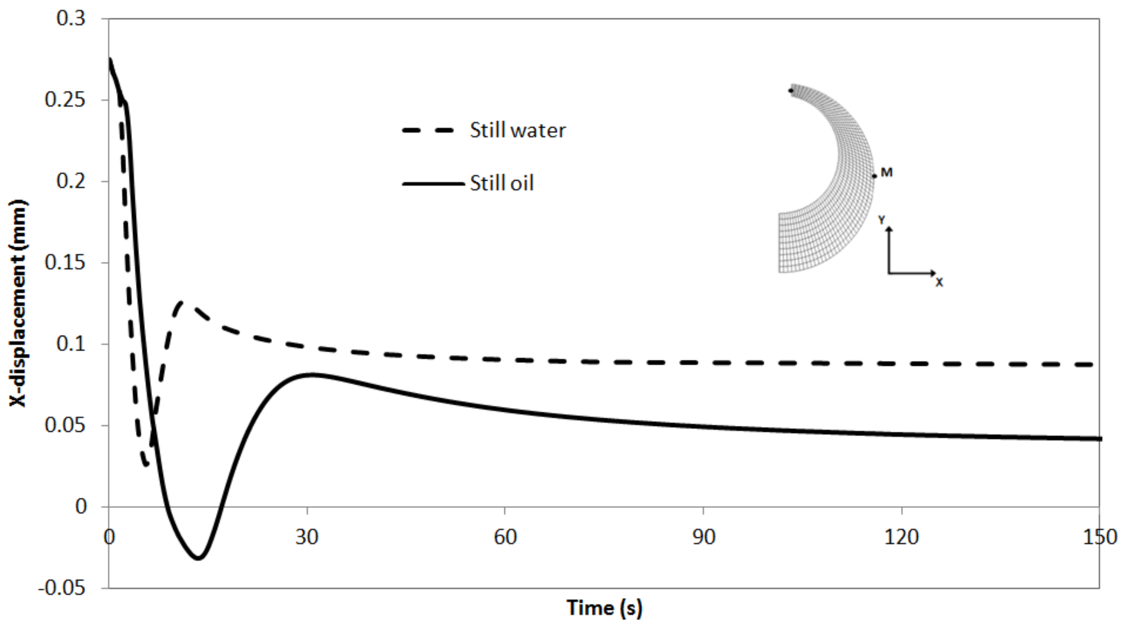

Figure 10 – Simulated displacements in the *x* direction for Node *M* of the C-ring for still oil and water quenching processes.

Table 2 – Simulated geometric distortions of the C-rings.

Dimensional changes	Simulation		Relative difference
	Still Oil	Still Water	
Gap opening (mm)	0.40	0.68	70%
Outside diameter (mm)	0.08	0.18	125%

Despite the larger distortion prediction of the water quenched C-ring when compared to the oil quenched C-ring, the experimental results showed that the C-ring cracks during water quenching process. This result indicates that the water quenched C-ring distortion prediction is not realistic. Table 3 presents a comparison between distortion prediction and experiments. A dye penetrant inspection was conducted in order to better visualize the water quenched C-ring cracks, as shown in Figure 11. The cracks can also be observed in Figure 12. Distortions and cracks caused by heat treatments may be controlled and/or avoided throughout proper selection of quenching media [12,13].

Table 3 – Dimensional changes for experiments and simulations (values in mm).

Quenchant	Experiments		Simulation		Prediction difference
	Gap opening	Outside diameter	Gap opening	Outside diameter	
Oil	0.43	0.09	0.40	0.08	6.5-6.7%
Water	cracked	cracked	0.68	0.18	-

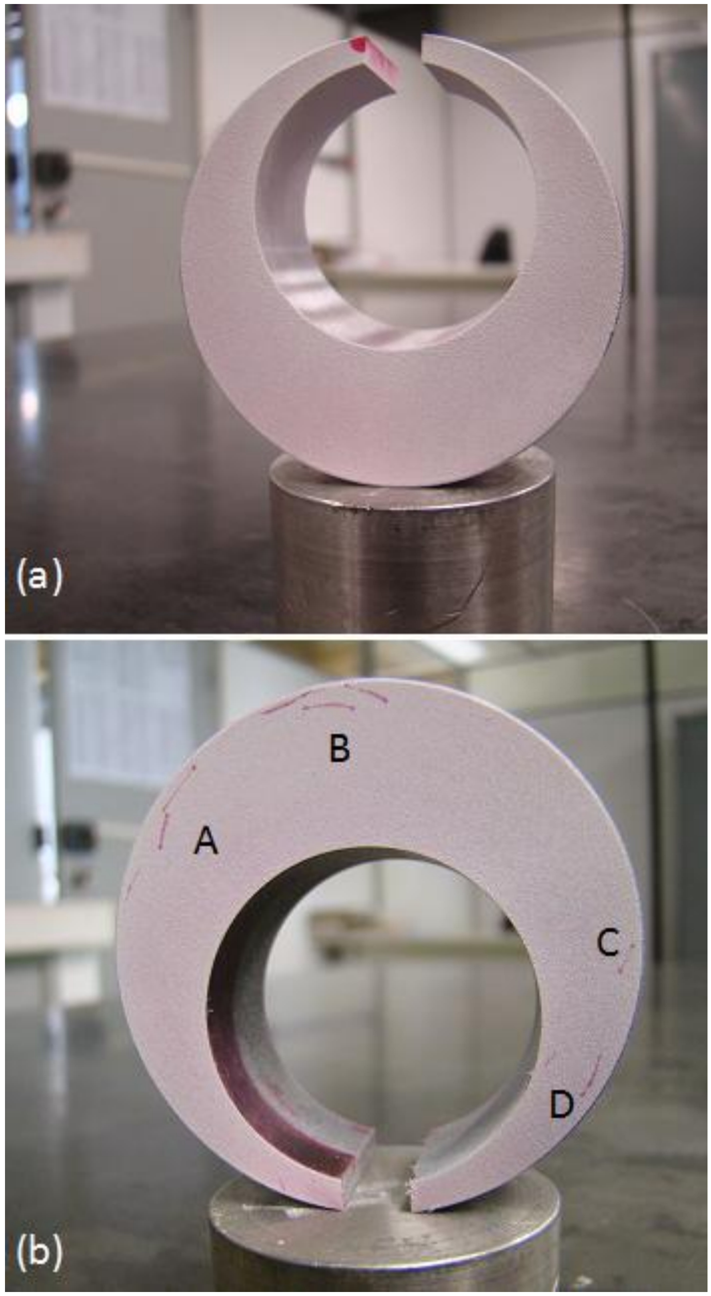

Figura 11 – Dye penetrant inspection (a) before and (b) after water quenching process; the C-ring presented cracks on regions A, B, C e D.

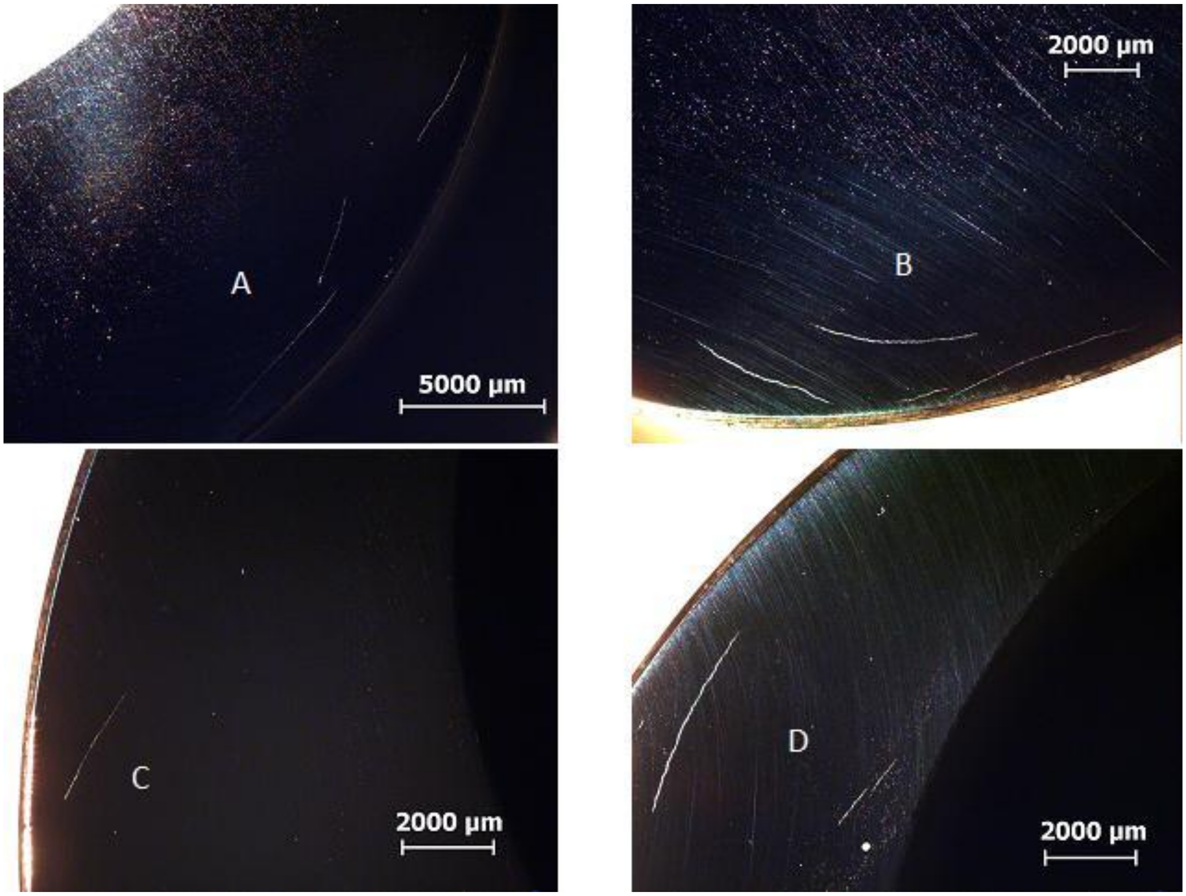

Figura 12 – Water quenched C-ring cracks.

3.2. Microstructure and hardness

Figure 13 shows the simulated distribution of martensite on the C-ring surface. The specimen was initially thermally expanded and austenitized. Starting at 4 s after the quench initiation, it is possible to observe in Figure 13 the beginning of martensite formation in the region close to the C-ring gap. After 10 s, practically all thermal expansion is absent, but martensite formation is still in progress, being now responsible for further ring distortions. The situation after 25 s of cooling shows that the martensite formation in the thicker portion of the C-ring is associated with the final opening of the ring gap and of the external diameter of the ring.

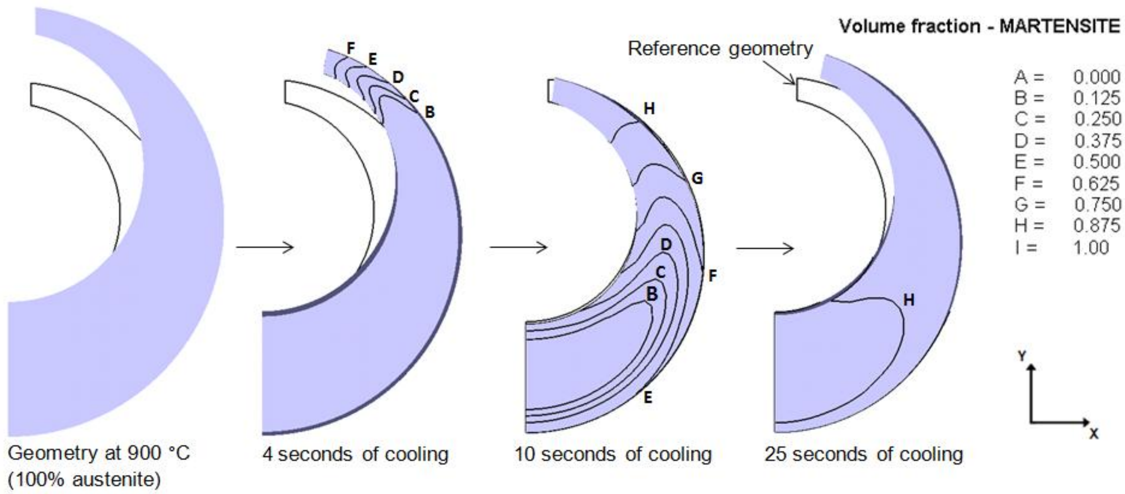

Figure 13 – Martensite formation on the C-ring during the cooling simulation (displacement magnified 20x).

Figure 14 displays the simulated results for the evolution of martensite volume fraction on the cross-section of the C-ring. High volume fractions of martensite are predicted. Starting at 4 s after the quench initiation, it is possible to observe the beginning of martensite formation in the region close to the C-ring gap. After 10 s, practically all thermal expansion is absent, but martensite formation is still in progress, being now responsible for further ring distortions. The situation after 25 s of cooling shows that the martensite formation in the thicker portion of the C-ring is associated with the final opening of the ring gap and of the external diameter of the ring. The literature indicates that martensite formation is of importance in quench distortion [14], and that the distortion happens during the early stages of the quenching process [6,11], as predicted in this work. The distortion magnitude may vary according to the C-ring material and dimensions and quenching characteristics. The material hardness values taken on the points defined in Figure 3 lie between 54 and 55 HRC after oil quenching, and between 57 and 59 HRC for water quenching process. The experimental microstructure analysis is shown in Figures 15-18.

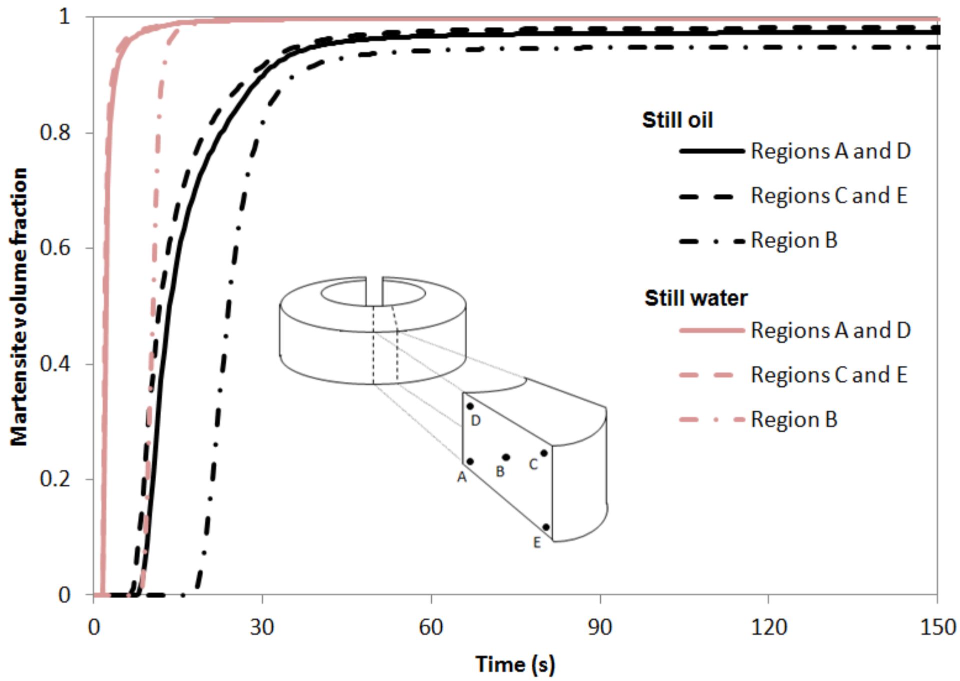

Figure 14 – Simulated evolution of the martensite volume fraction at several points in the transversal cross-section of the C-ring during oil quenching.

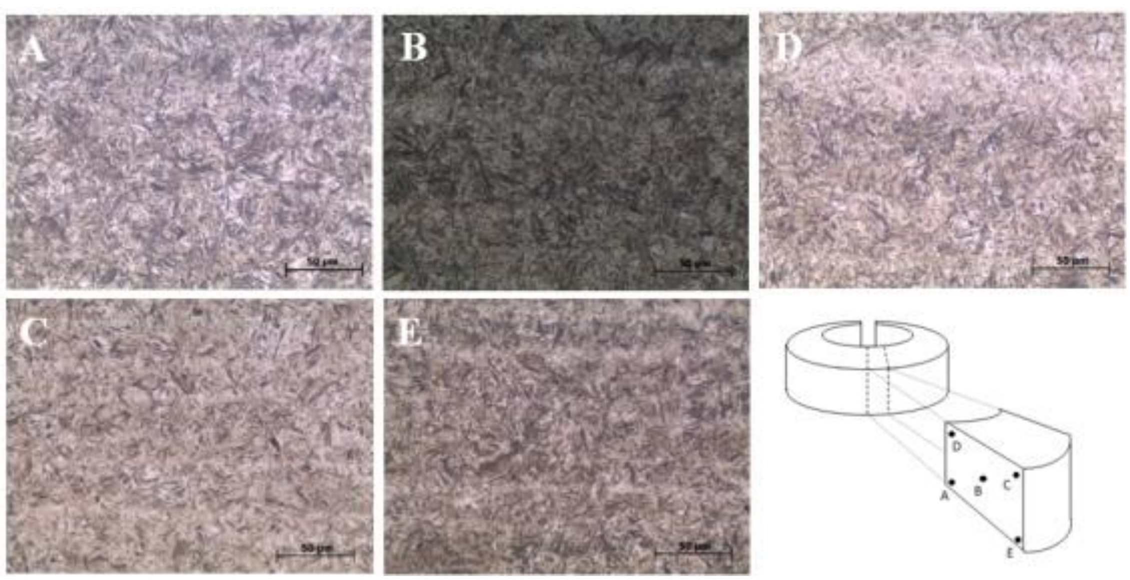

Figure 15 – Micrographs from various points in the transversal cross-section of the oil quenched C-ring, indicating the presence of martensite in all locations (optical microscopy).

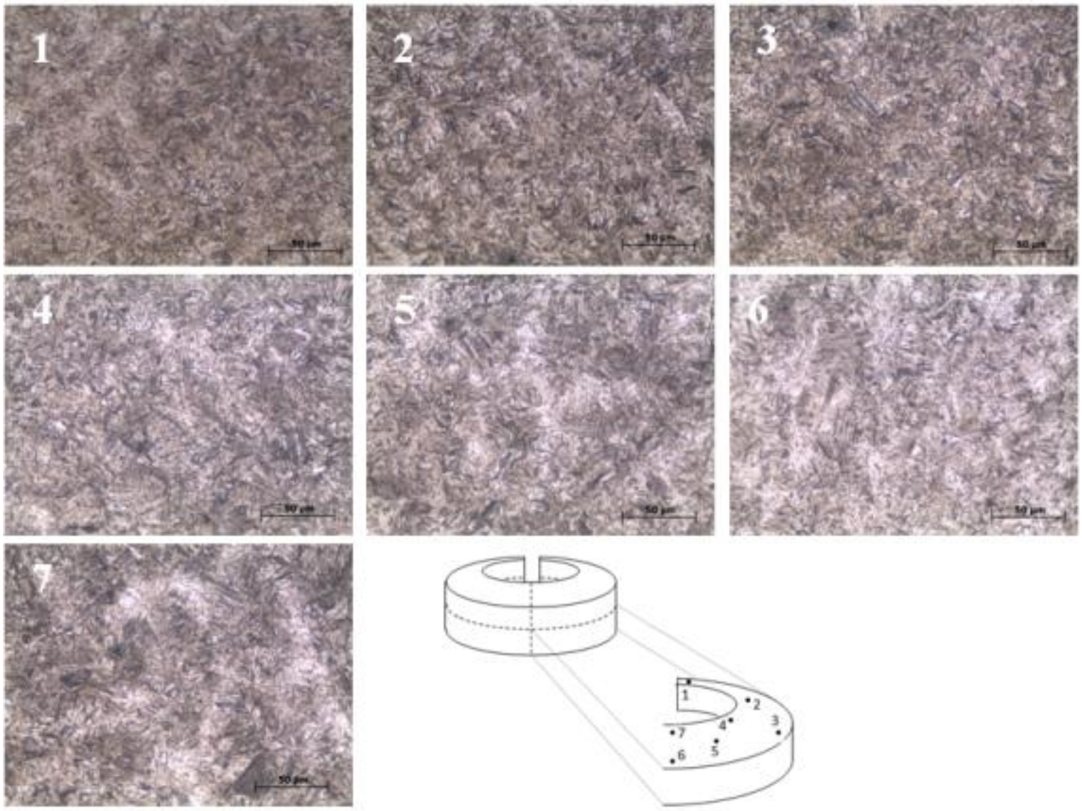

Figure 16 – Micrographs from various points in the longitudinal cross-section of the oil quenched C-ring, indicating the presence of martensite in all locations (optical microscopy).

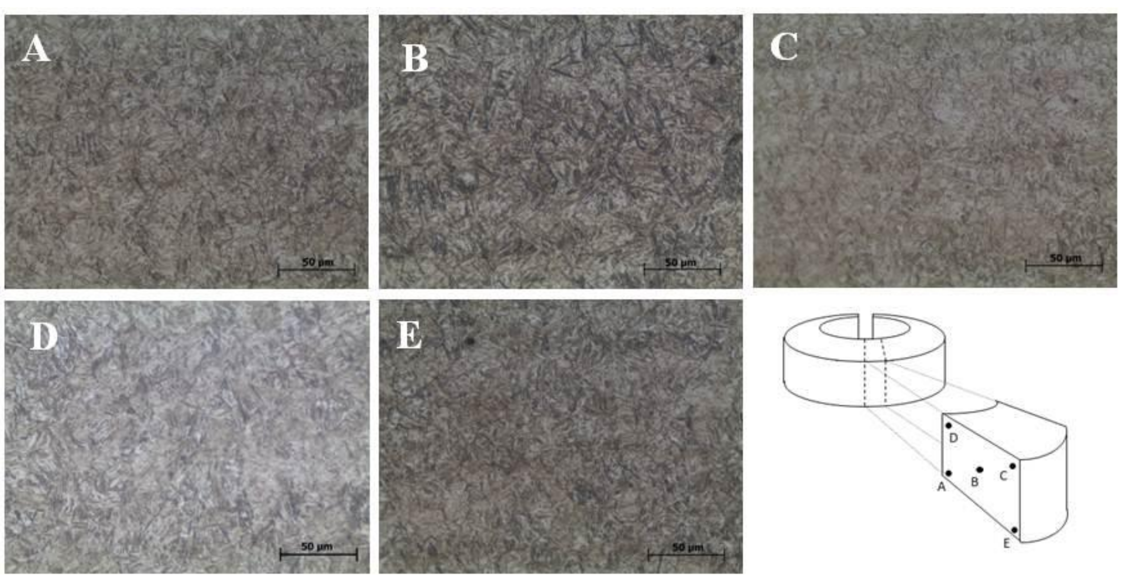

Figure 17 – Micrographs from various points in the transversal cross-section of the water quenched C-ring, indicating the presence of martensite in all locations (optical microscopy).

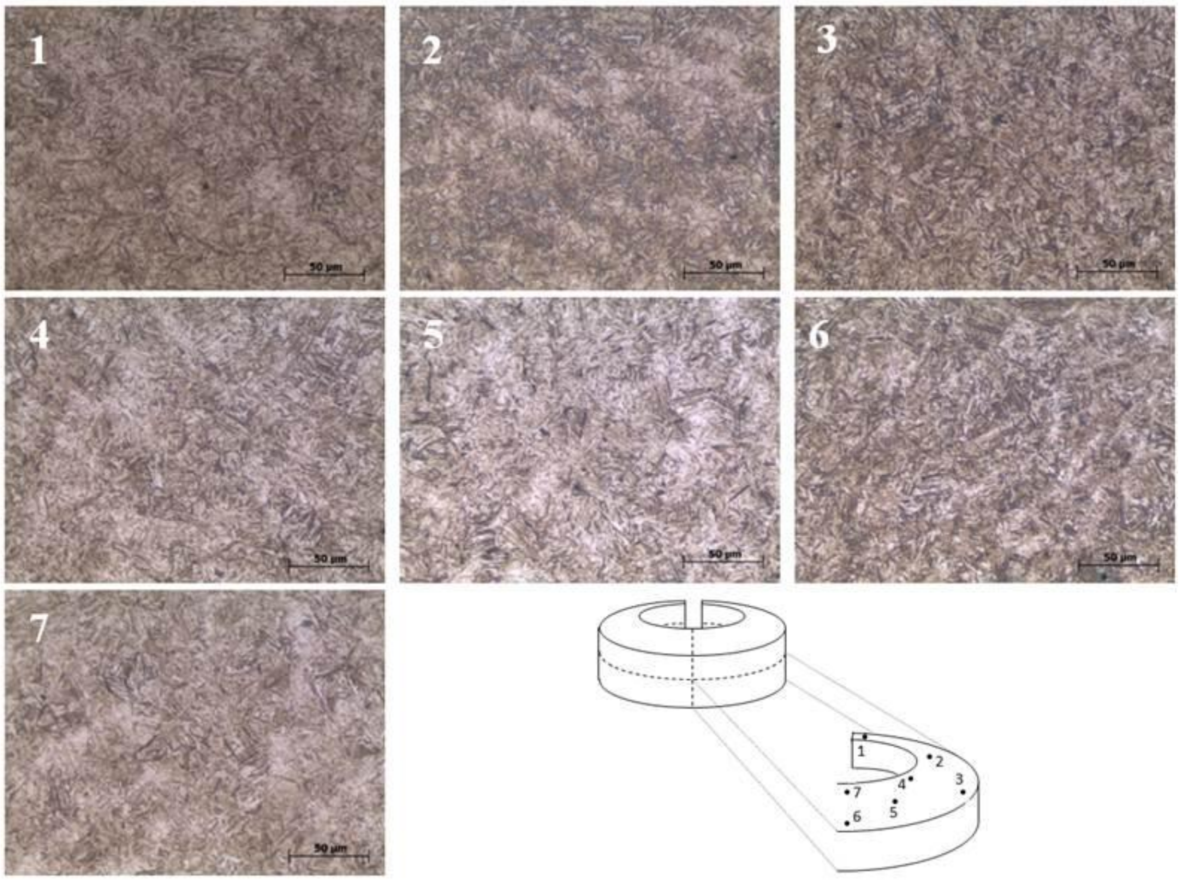

Figure 16 – Micrographs from various points in the longitudinal cross-section of the oil quenched C-ring, indicating the presence of martensite in all locations (optical microscopy).

4 CONCLUSIONS AND OUTLOOK

The simulation of quenching, using the DEFORM™ software and thermo-physical material data from JMatPro, led to the validated prediction of final microstructures, hardness and distortion magnitudes. The volume fraction of martensite at the end of the process is above 95% for any material region in the C-ring. The final hardness prediction was 56 HRC for oil quenching and 58 HRC for water quenching.

According to the simulation, the geometric distortion of the C-ring is associated with the austenite to martensite transformation at the thickest part of the ring, during the final stages of the quenching process.

The water quenching process has provided larger predicted distortion values due to its higher severity when compared to the oil quenching process. However, the C-ring has cracked during water quenching experiments.

The methodology used to predict quench distortion may be applied to parts of various shapes and materials. Therefore, the heat treatment process may be included in the process design to obtain the final product dimension.

Residual stresses at the cracking regions should be investigated in order to better understand the phenomena.

REFERENCES

[1] CANALE, L. C. F.; TOTTEN, G. E. Overview of distortion and residual stress due to quench processing part I: factors affecting quench distortion. International Journal of Materials and Product Technology; v.24; Nos.1-4; 4-52; 2005.

[2] HOWES, M. A. Factors affecting distortion in hardened steel components: I. The International Journal of Thermal Technology; October, 65-70, 1993.

[3] HOWES, M. A. Factors affecting distortion in hardened steel components: II. The International Journal of Thermal Technology; December, 30-32, 1993.

[4] GONZALEZ-MENDEZ, J. L. et al. Distortion in rolled and heat-treated rings. The International Journal of Forging Business & Technology; February, 12-15, 2012.

[5] NARAZAKI, M.; TOTTEN, G. E. Distortion of heat treated components. In: TOTTEN, G. E., editor. Steel heat treatment: metallurgy and technology. Boca Raton: Taylo & Francis Group, LLC; p. 608-650, 2006.

[6] FUKUZUMI, T.; YOSHIMURA, T. Reduction of distortion caused by heat treatment on automobile steel gear. Proceedings of the First International Conference on Quenching & Control of Distortion, Chicago, USA; 199-203, 1992.

[7] BOYLE, E.; BOWERS, R.; NORTHWOOD, D. O. The use of navy c-ring specimens to investigate the efects of initial microstructure and heat treatment on the residual stress, retained austenite, and distortion of carburized automotive steels. SAE International; 31-39; 2007.

[8] CYRIL, N. et al. Comparison of experimental and simulation distortions of quenched C-ring test parts. International Journal of Material Forming; 2, 263-266, 2009.

[9] TOTTEN, G. E.; BATES, C. E.; CLINTON, N. A. Handbook of Quenchants and Quenching, ASM International, Materials Park; pp. 485-492, 1993.

[10] GRUM, J.; BOZIC, S.; ZUPANCIC, M. Influence of quenching agents on distortion of modified navy C-rings made of heat-treatment steel 4140. Proceedings of the 8th Seminar of the International Federation for Heat Treatment and Surface Engineering, Dubrovnik-Cavtat, Croatia; 145-155; 2001.

[11] HARDIN, R. A.; BECKERMANN, C. Simulation of Heat Treatment Distortion. Proceedings of the 59th SFSA Technical and Operating Conference; 3.3, 1-32, 2005.

[12] LUO, X.; TOTTEN, G. E. Analysis and prevention of quenching failures and proper selection of quenching media: an overview. Journal of ASTM International; v.8, n.4, 1-29, 2011.

[13] ESHRAGHI-KAKHKI, M.; GOLOZAR, M. A.; KERMANPUR, A. Application of polymeric quenchant in heat treatment of crack-sensitive steel mechanical parts: modeling and experiments. Materials & Design; 32, 2870-2877, 2011.

[14] AMEY, C. M.; HUANG, H.; RIVERA-DÍAZ-DEL-CATILLO, P. E. J. Distortion in 100Cr6 and nanostructured Bainite. Materials & Design; 35, 66-71, 2012.